Desalination and Water Treatment
www.deswater.com
doi: 10.5004/dwt.2020.25897

195 (2020) 341–352
August

Efficient removal of malachite green dye from aqueous solution using *Curcuma caesia* based activated carbon

Charu Arora[a,*], Pramod Kumar[a], Sanju Soni[a], Jyoti Mittal[b], Alok Mittal[b], Bhupender Singh[c]

[a]*Department of Chemistry, Guru Ghasidas University, Bilaspur – 495009, CG, India, emails: charuarora150@gmail.com (C. Arora), chemggv@gmail.com (P. Kumar), sanjusoni87@gmail.com (S. Soni)*
[b]*Department of Chemistry, Maulana Azad National Institute of Technology, Bhopal, India, emails: jyalmittal@yahoo.co.in (J. Mittal), aljymittal@yahoo.co.in (A. Mittal)*
[c]*Institute Instrumentation Centre, Indian Institute of Technology Roorkee, Roorkee – 247667, India, email: bsinghiitr@gmail.com (B. Singh)*

Received 19 September 2019; Accepted 27 March 2020

ABSTRACT

Ash of *Curcuma caesia* has been explored as potential adsorbent for removal of hazardous dye malachite green from aqueous solution. Surface morphology of ash was studied using scanning electron microscopy. The adsorption mechanism and kinetics of the process have been investigated. Adsorption process is pH-dependent and favored at basic pH. Dubinin–Radushkevich (D–R) adsorption model has been found to be most appropriate for the adsorption. Physic-sorption has been found to control the adsorption mechanism. Intraparticle diffusion is best followed. Batch and column adsorption studies of malachite green onto *C. caesia* ash were carried out. Adsorption capacity for the column process is found to be 38.16 mg/g which is less than that of the batch process. Value for change in Gibbs free energy is negative over the entire temperature range, indicating the process to be spontaneous. The adsorption process is endothermic.

Keywords: Malachite green; Adsorption isotherms; Adsorption kinetics; Dye removal; *Curcuma caesia*

1. Introduction

Rapid industrial development has led to excessive use of synthetic dyes in various industries viz. paper, textile, leather, plastic, food, cosmetics, and pharmaceuticals to color the products, resulting in a continuous discharge of dye contaminants into the water bodies causing water pollution. Complex aromatic structures of synthetic dyes provide them thermal, optical, and physicochemical stability. Therefore, the biological degradation of these dyes is difficult [1,2]. Most of the synthetic organic dyes are toxic and carcinogenic in nature thus have a severe impact on the environment and living beings [3,4]. Therefore, a study on dye removal has become the area of immense scientific interest. There are several reported methods viz., photochemical degradation, chemical oxidation, biological degradation, coagulation, reverse osmosis, flotation, electrochemical treatment, adsorption, etc., which are used for dye removal study [2,3,5,6]. Among these methods, adsorption is most advantageous due to its effectiveness and economy. Number of materials viz., coal, wood, rice husk, fly ash, activated carbon, cotton waste, clay, and other porous materials have been used for the adsorptive removal of dye from its aqueous solutions [7–11]. It is also well-known that during the combustion of biomass or biomass/coal blends, the large amounts of alkali metals and alkaline earth metals in biomass or coal can also result in severe ash-related problems [12–14].

A basic cationic dark green colored dye, named Malachite Green (MG) has enormous industrial applications in paper, plastic, textile, and pharmaceutical industries. It has also been used as a strong anti-fungal, anti-bacterial,

* Corresponding author.

and anti-parasitical agent in fish farming. It has highly mutagenic, teratogenic, chromosomal fractures, and carcinogenic effects due to the presence of nitrogen in its complex aromatic structure [5,15,16]. Several adsorbents like bentonite, activated carbon, neem sawdust, rattan sawdust, carbon, halloysite nanotubes, natural zeolite, modified rice husk, degressed coffee bean, and treated ginger waste have been reported for MG removal from solutions [5]. We are reporting for the first time, efficient and fast dye removal using activated carbon of *Curcuma caesia*.

C. caesia (commonly known as black turmeric or kali haldi belongs to the *Zingiberaceae* family), is a perennial herb with bluish-black rhizomes. It is available throughout the northeast, central India, Papi hills of east Godavari, west Godavari, and Andhra Pradesh. It possesses various medicinal properties such as anti-fungal activity, smooth muscle relaxant, anti-asthmatic activity, bronchodilating activity, antioxidant activity, anxiolytic, and central nervous system depressant activity, locomotor depressant, anti-convulsant, anthelmintic activity, anti-bacterial, anti-ulcer, and anti-mutagenic activities [17–19]. The rhizomes are used in the treatment of hemorrhoids, leprosy, asthma, epilepsy, fever, wound, vomiting, menstrual disorder, tumor, piles, aphrodisiac, inflammation, gonorrhoeal discharges. The inner part of the rhizome of black turmeric is of bluish-black color and emits a characteristic sweet aroma, due to presence of essential oil [17]. Indian tribal women use the powder of rhizomes as a face-pack during their engagement and marriage period. Crushed fresh rhizomes provide relief from migraines when applied as a paste on the forehead. Fresh rhizomes are also used in the treatment of snake and scorpion bites [18,20].

In research labs, batch experiments are generally carried out for dye removal study from aqueous solutions in tiny quantity. The batch technique is a simple technique and it provides a simple way to elucidate the parameters influencing the adsorption process [21–23]. However, large volumes of wastewater are produced in industries. Therefore, batch adsorption study is not sufficient for practical application of the adsorbent for dye removal. To overcome this issue, column technique is applied in which the adsorbent is constantly in contact with spanking fresh solution. Column technique is helpful in deciding the amount of adsorbent required for removal of pollutants from wastewater. Efficiency of column technique can be explained via breakthrough curve. A plot showing relationship between column effluent concentration and either time of treatment or volume treated is known as Breakthrough curve [24]. In the present work both the techniques, that is, batch and column adsorption processes are employed for the removal of malachite green from aqueous solution using ash of *C. caesia.*

2. Experimental section

2.1. Development of adsorbent ash

In the dye removal study, ash of *C. caesia* was used as adsorbent. Fresh Bluish black rhizome of *C. caesia* was procured from Kandhmal, Odisa, India. The collected rhizomes were sun-dried and powdered. The powdered rhizomes are converted into ash by heating in a muffle furnace at 550°C for 5 h. After cooling, the ash is collected and used without further chemical treatment.

2.2. Materials and characterization methods

Malachite green (MG) dye was procured from Merck, India. A stock solution of 100 gm/L of MG dye was prepared using distilled water. Subsequent solutions were prepared by diluting the stock solution. Dye removal study had been carried out spectrophotometricaly. Effect of various parameters on dye adsorption was studied using 10 mL dye solution and remaining dye concentration was investigated by recording absorbance at 617 nm (λ_{max}). Studies were carried out using Shimadzu UV 1800 spectrophotometer (Kyoto, Japan). Scanning electron microscopy (SEM) micrographs of the adsorbent before and after adsorption were recorded using Merlin VP Compact (Carl ZEISS Germany make) having airlock chamber. The IR spectrum of the adsorbent was carried out using Nicolet iS10, Thermo Fisher Scientific Instrument, Madison, USA, OMNIC 9 and TQ analysis software packages Fourier transform infrared spectrometer. Zeta potential of the adsorbent suspended in aqueous solution was determined using a zeta-sizer Nano-ZS (Malvern) at room temperature. The characterization of the adsorbent was done by adopting strategies similar to earlier studies [25,26].

2.3. Dye adsorption study

Batch adsorption experiments were carried out with 10 mL MG dye solution for 2–12 mg/L initial dye concentrations, 1–5 mg of adsorbent, 4–9 pH, 5–35 min contact time, and 30°C–45°C temperature. pH of dye solution was adjusted by adding dilute solutions of HCl and NaOH. Dye concentration was analyzed spectrophotometricaly by UV-vis spectrophotometer at maximum wavelength (λ_{max}) 617 nm in absorbance mode.

The R (removal efficiency, %), Q_t (amount of dye adsorbed at time t, mg/g), and Q_e (amount of dye adsorbed at equilibrium, mg/g) were calculated from the following equations, respectively.

$$R = \frac{\left(C_0 - C_e\right) \times 100}{C_0} \tag{1}$$

$$Q_t = \frac{\left(C_0 - C_t\right) V}{m} \tag{2}$$

$$Q_e = \frac{\left(C_0 - C_e\right) V}{m} \tag{3}$$

where C_0, C_t, and C_e (mg/L) are the concentrations of dye solutions at initial, at time t and equilibrium, respectively, V (L) is the volume of the dye solution, and m (g) is the amount of adsorbent used.

2.4. Column adsorption study

Column experiment was conducted in a glass column having 19 cm length, 0.5 cm diameter, and 0.25 g adsorbent

mass. The adsorbent was filled a fixed bed height: 1 cm and cross-sectional area: 0.2 cm^2 on a cotton wool support. The solution with 10 mg/L MG dye content was passed in the downflow mode through the column with linear flow rate of 1.2 mL/min. Aliquots of 6.0 mL effluent solutions were collected at regular time interval of 5 min and analyzed spectrophotometrically for dye content.

The breakthrough curve [27] is plotted in terms of C_t/C_0 vs. time, where C_t is the concentration of effluent at time t and C_0 is the initial concentration influent dye solution. The volume of effluent, V_{ef} can be calculated by using the following formula:

$$V_{ef} = vt \tag{4}$$

where t (min) is the flow time and v (mL/min) is the flow rate.

Amount of dye adsorbed at time t, Q_{total} (mg) can be represented by area under the breakthrough curve, which can be determined by the integration (calculated using software OriginPro 8).

$$Q_{total} = v\int_{t=0}^{t=t}\left(C_0 - C_t\right)dt \tag{5}$$

The total amount of dye (m_{total}) sent to the column at time t can be calculated by:

$$m_{total} = C_0 vt \tag{6}$$

The dye removal R (%) can be calculated as:

$$R = \frac{Q_{total}}{m_{total}} \times 100 \tag{7}$$

The adsorption capacity of the adsorbent q_t (mg/g) at time t can be obtained by the use of following equation (calculated using software OriginPro 8).

$$q_t = \frac{v\int_{t=0}^{t=t}\left(C_0 - C_t\right)dt}{m} \tag{8}$$

where m is the amount of adsorbent used in column.

3. Results and discussion

3.1. Characterization of adsorbent

SEM image of the adsorbent is shown in Fig. 1 which reveals porous structure of activated carbon of *C. caesia* rhizomes which may favor the adsorption process. Powder X-ray diffraction (PXRD) pattern of the adsorbent is shown in Fig. S1 which reveals the peaks at 2q angles 26.7°, 28.6°, 30.5°, 32.8°, 34.1°, 40.64°, 43.4°, and 45.1°. X-ray diffraction (XRD) pattern was found to remain unchanged after every cycle (after desorption) till the eighth cycles. IR spectra (Figs. S2 and S3) of *C. caesia* ash before and after adsorption also confirm the adsorption process.

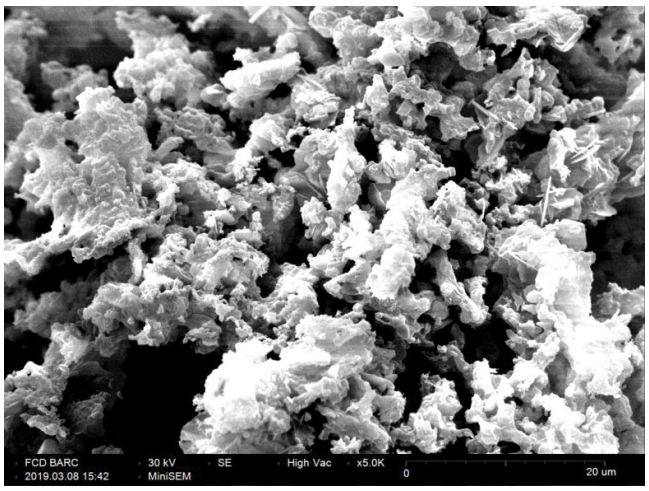

Fig. 1. SEM micrograph of ash of *Curcuma caesia* adsorbent.

3.2. Impact of initial dye concentration and contact time

Impact of initial dye concentration at various contact time on MG dye removal using *C. caesia* ash is shown in Fig. 2. The results reveal that removal of dye as well as uptake capacity increase as the initial concentration of MG dye increases from 2 to 12 mg/L. The increase in the uptake capacity is probably due to the increase in the mass gradient between the dye solution and ash of *Curcuma caesia* as the initial dye concentration increases [28].

3.3. Impact of adsorbent dose

Impact of dose of adsorbent on adsorption capacity was studied and the results obtained are represented in Fig. 3. The results indicate increase in contact surface area and exchangeable sites on an increasing amount of adsorbent lead to increase in the percentage dye removal [29].

3.4. Impact of pH of dye solution

Experiments for the impact of pH on adsorption were carried out by adjusting the pH range between pH 4–9. The experimental data indicated that the dye removal was so effective at higher pH (Fig. 4a) which can be explained on the basis of protonation and deprotonation of MG dye in acidic and basic medium, respectively. At a lower pH, the dye molecule has high positive charge density due to presence of excess H^+ ions, suggesting the existence of repulsion between the positively charged surface and the positively charged dye molecule. Therefore, lower adsorption of dye molecules. On contrary, in the basic medium the formation of electric double layer changes its polarity, and consequently the dye uptake increases [15].

On the other hand, effect of initial pH of dye solution can be explained by surface charge of the adsorbent which was determined by zeta potential. As shown in Fig. 4b, the adsorbent has positive zeta potential at lower pH indicating the positive surface charge which turns negative as the pH increases. In higher pH ranges the adsorbent surface carries negative charge which benefits the adsorption

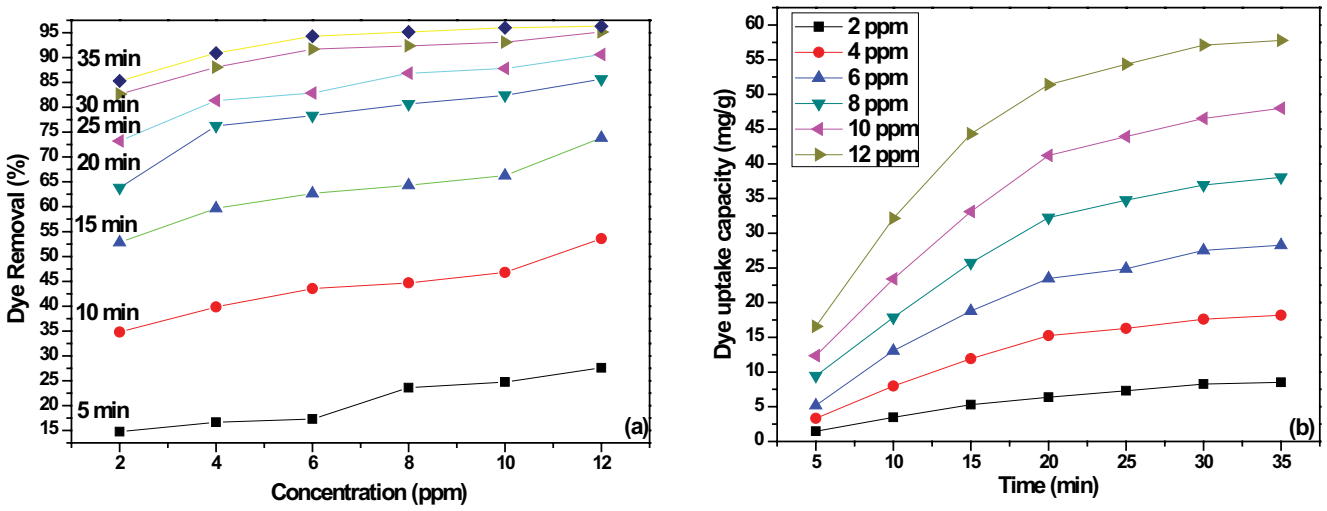

Fig. 2. Impact of (a) initial dye concentration and (b) contact time on removal of Malachite green.

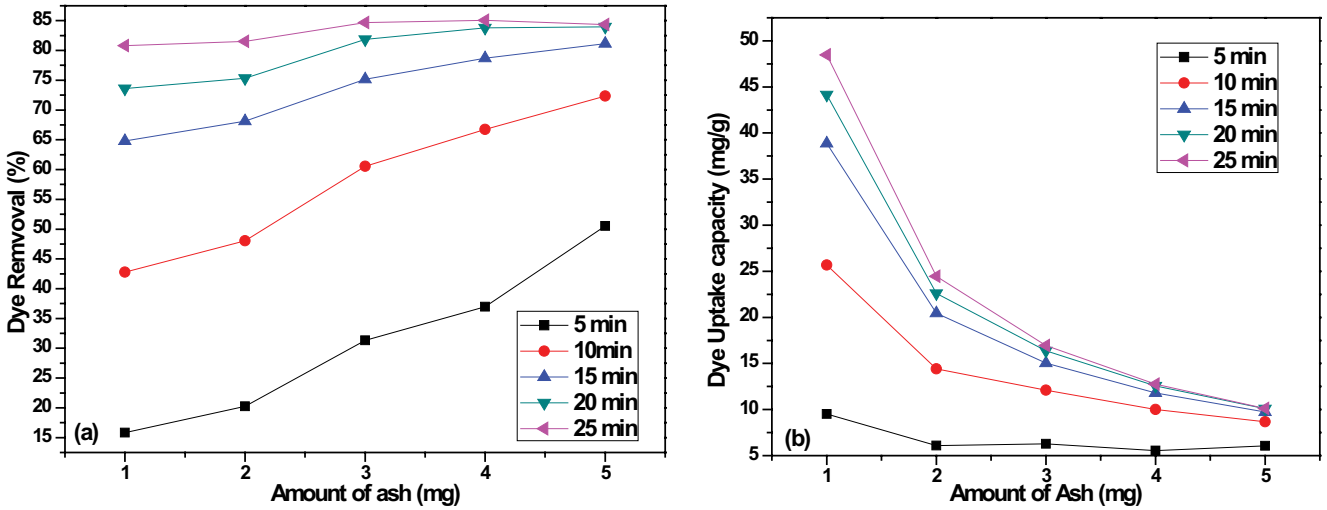

Fig. 3. Effect of adsorbent dose on (a) removal of Malachite green and (b) dye uptake capacity of adsorbent.

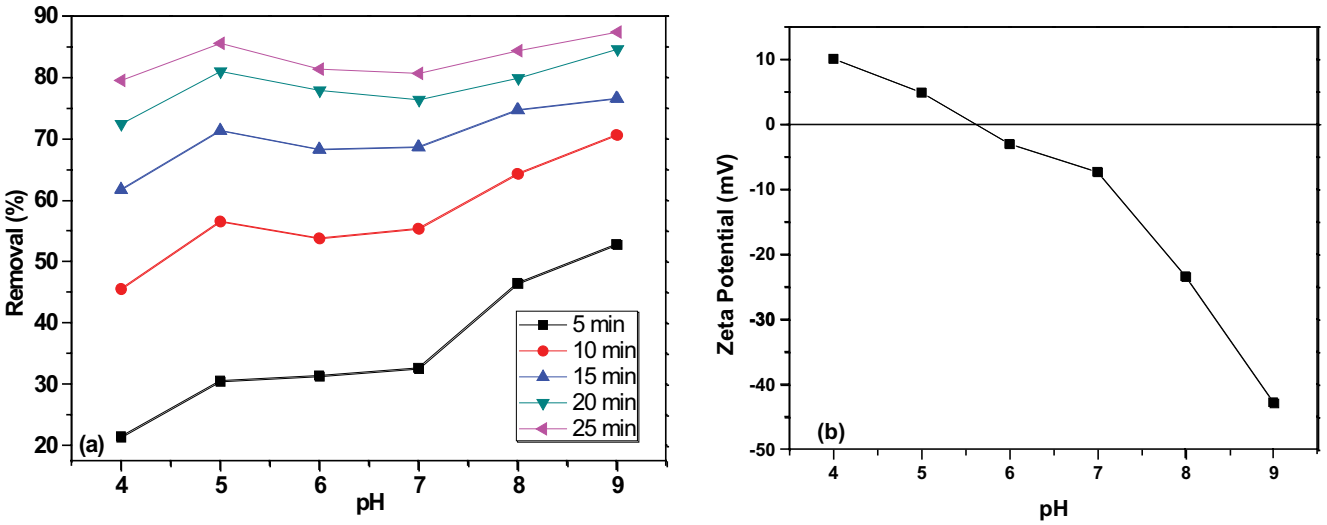

Fig. 4. Effect of pH of dye solution on (a) removal of Malachite green and (b) zeta potential of ash of *curcuma caesia.*

of cationic MG dye through electrostatic interaction. Therefore, adsorption rate were improved with increasing pH values [30,31].

3.5. Impact of temperature

Dye removal was examined at several temperatures range started from 30°C to 45°C and the result obtained is shown in Fig. 5. As the experimental temperature ascends, the dye molecules diffuse more quickly resulting in greater opportunity to connect with adsorbent through specific sites. As a result, more dye molecules get adsorbed by the adsorbent at higher temperature [32].

3.6. Thermodynamic parameters

Thermodynamic parameters viz., $\Delta H°$ (change in enthalpy), $\Delta S°$ (change in entropy), and $\Delta G°$ (change in Gibb's free energy) can be calculated by the following equations:

$$\ln\left(\frac{mQ_e}{C_e}\right)=\frac{\Delta S}{R}-\frac{\Delta H}{RT} \tag{9}$$

$$\Delta G=\Delta H-T\Delta S \tag{10}$$

where Q_e and C_e are the equilibrium concentration of dye on the adsorbent and in the solution, respectively. T is the temperature and R is the gas constant [33]. Plot of $\ln(mQ_e/C_e)$ vs. $1/T$ (Fig. 6) gives the value of entropy and enthalpy. The obtained values of the parameters are presented in Table 1. Spontaneous nature and feasibility of the adsorption process can be explained by negative values of free energy ($\Delta G°$) [29]. Increase in absolute values of free energy with temperature suggests that the adsorption is favorable at higher temperature [16]. An increase in randomness at the solid-solution interface during the adsorption is indicated by the positive value of $\Delta S°$.

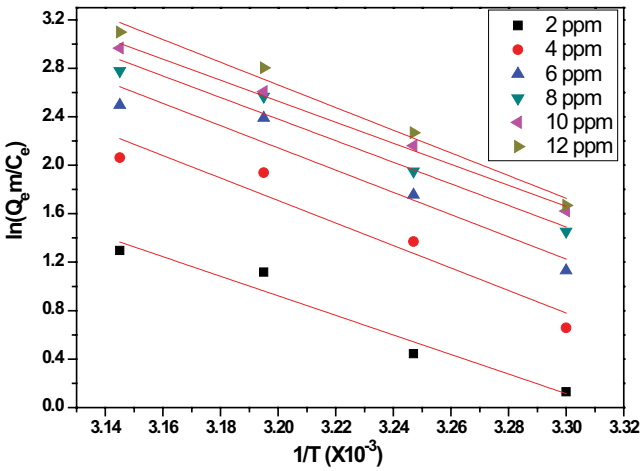

Fig. 6. Linear plot of $\ln(mQ_e/C_e)$ vs. $1/T$ to give thermodynamic parameters.

Endothermic and chemisorption process of adsorption is again confirmed by the positive value of $\Delta H°$ which is higher than 40 kJ/mol [34].

3.7. Adsorption isotherm study

Four adsorption isotherm models viz., Freundlich, Langmuir, Temkin, and Dubinin–Radushkevich (D–R) isotherm models were applied and evaluate to explain the adsorption mechanism. In Freundlich adsorption isotherm, adsorption takes place in a heterogeneous surface having uniform distribution of adsorption heat over the surface [35]. On the other hand, Langmuir isotherm was derived by assuming the adsorbent is homogeneous, both surface and bulk phases reveal ideal behavior and the adsorption is monomolecular [36]. Temkin isotherm model considers effect of some indirect adsorbent–adsorbate interaction and suggests that there is linear decrease in heat of adsorption of all the

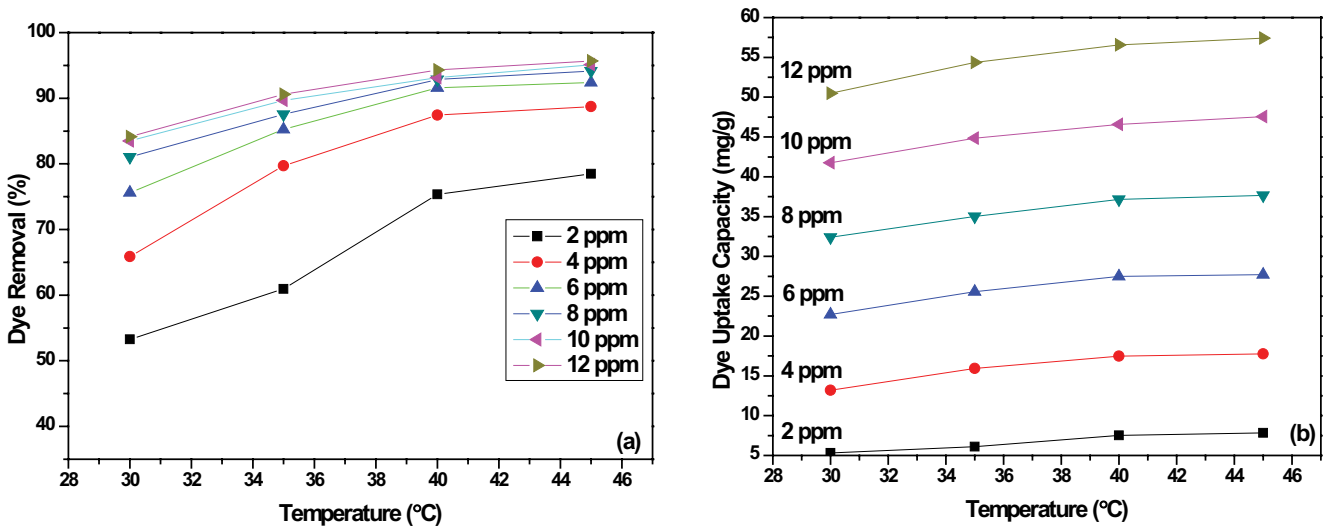

Fig. 5. Effect of temperature on (a) removal of Malachite green and (b) dye uptake capacity of adsorbent.

Table 1
Thermodynamic parameters for adsorption of malachite green on *Curcuma caesia* ash

Dye con-centration	$\Delta H°$ (kJ/mol)	$\Delta S°$ (kJ/mol/K)	$\Delta G°$ (kJ/mol) at temperatures			
			303 K	308 K	313 K	318 K
2	72.133	0.252	–4.175	–5.434	–6.693	–7.952
4	67.089	0.222	–0.284	–1.396	–2.507	–3.619
6	77.154	0.261	–1.959	–3.264	–4.57	–5.875
8	76.309	0.262	–3.079	–4.389	–5.699	–7.009
10	73.998	0.257	–3.747	–5.03	–6.313	–7.596
12	77.759	0.271	–4.344	–5.699	–7.053	–8.408

molecules in the layer with coverage [37]. The D–R model can suitably explain the adsorption behavior on both homogeneous and heterogeneous surfaces at low concentration [38]. The linear forms of the isotherm models are given as follow:

Freundlich isotherm:

$$\ln Q_e = \ln K_f + \frac{1}{n}\ln C_e \tag{11}$$

Langmuir isotherm:

$$\frac{C_e}{Q_e} = \frac{1}{K_L Q_L} + \frac{C_e}{Q_L} \tag{12}$$

Temkin isotherm:

$$Q_e = \frac{RT}{b_T}\ln K_T + \frac{RT}{b_T}\ln C_e \tag{13}$$

D–R isotherm:

$$\ln Q_e = \ln Q_0 - \beta\varepsilon^2 \tag{14}$$

where n and K_f are adsorption intensity and Freundlich constant related to adsorption capacity. K_L and Q_L are Langmuir constants related to energy of adsorption and adsorption capacity. K_T is the Temkin parameter related to the equilibrium binding energy and b_T is the Temkin constant related to adsorption heat. B is the adsorption free energy, and ε is the Polanyi potential.

MG adsorption isotherms of activated carbon of *C. caesia* rhizomes at different temperatures are shown in Figs. 7–10 and the isotherm parameters are listed in Table 2. The models were evaluated by the adjusted determination factor (R^2). D–R model was more corresponded with the adsorption isotherm data than other isotherm models. Using the D–R isotherm parameters mean sorption energy E was calculated using the following formula and the obtained value is listed in Table 1:

$$E = \frac{1}{\sqrt{2\beta}} \tag{15}$$

Since the values of E at various temperatures (Table 2) are less than 8 kJ/mol, therefore physico-sorption controls the adsorption mechanism [39].

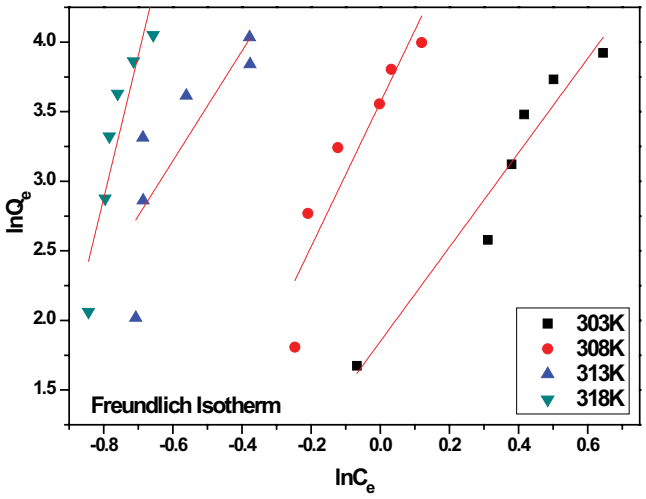

Fig. 7. Linear plot of Freundlich adsorption isotherm.

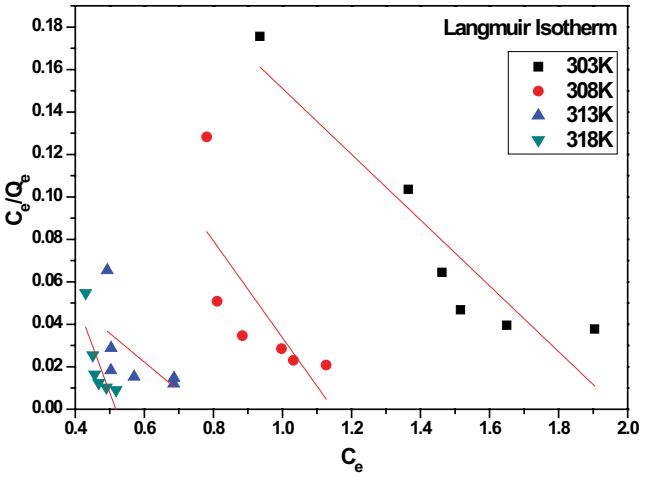

Fig. 8. Linear plot of Langmuir adsorption isotherm.

3.8. Rate constant study

In order to investigate the order of the ongoing adsorption process and also to evaluate the specific rate constant three kinetic models like Lagergren's pseudo-first-order, Ho's pseudo-second-order and Morris intraparticle diffusion

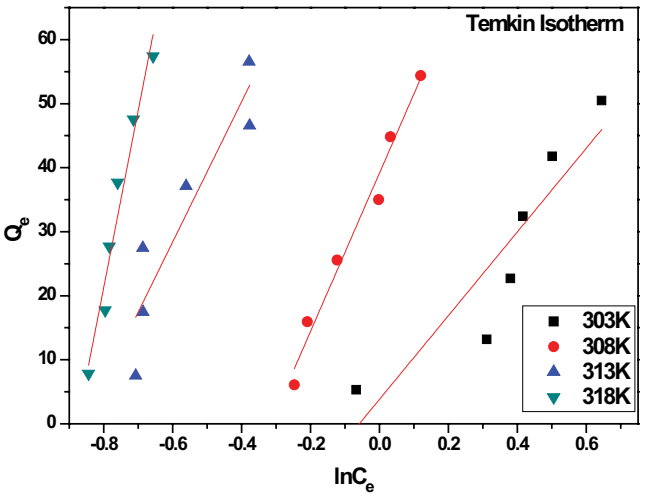

Fig. 9. Linear plot of Temkin adsorption isotherm.

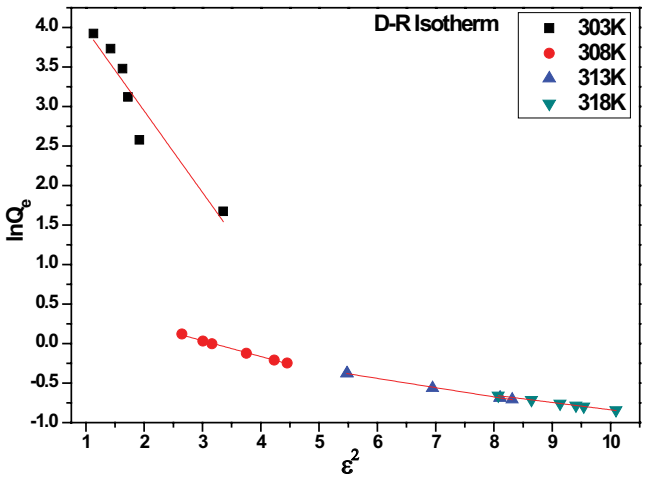

Fig. 10. Linear plot of D–R adsorption isotherm.

Table 2
Isotherm parameters for adsorption of malachite green on *Curcuma caesia* ash

S. No.	Adsorption isotherms		Parameters at temperatures			
			303 K	308 K	313 K	318 K
1	Freundlich isotherm	$1/n$	3.392	5.183	3.951	10.258
		n	0.294811	0.192938	0.2531	0.097485
		K_f	6.35346	35.4102	248.887	65186
		R^2	0.928	0.827	0.6	0.805
2	Langmuir isotherm	Q_L	–6.451613	–4.385965	–7.352941	–2.267574
		K_L	–0.5065	–0.8702	–1.3077	–1.9342
		R^2	0.832	0.461	0.213	0.533
3	Temkin isotherm	b_T	38.5349	20.71153	23.75689	9.582333
		K_T	1.06043	1.37283	2.36157	2.40429
		R^2	0.796	0.974	0.826	0.949
4	D–R isotherm	β	1.03	0.201	0.117	0.093
		Q_0	149.157	1.89459	1.29823	1.09308
		E	0.697	1.577	2.067	2.319
		R^2	0.894	0.996	0.999	0.999

model were employed. Linear equations for all the three models are given as following respectively [33]:

$$\ln\left(Q_e - Q_t\right) = \ln Q_e - k_1 t \tag{16}$$

$$\frac{t}{Q_t} = \frac{1}{k_2 Q_e^2} + \frac{t}{Q_e} \tag{17}$$

$$Q_t = k_i t^{0.5} + C \tag{18}$$

where Q_e and Q_t are the amount of dye adsorbed at equilibrium and time t, respectively. k_1, k_2, and k_i are the rate constants of adsorption for pseudo-first-order, pseudo-second-order, and intraparticle diffusion models, respectively. C is a constant related to the thickness of boundary layer [38].

For the present study, linear plots of all the kinetic models are shown in Figs. 11–13. Parameters corresponding to the kinetic models are listed in Table 3. Intraparticle diffusion was best followed by the adsorption of MG onto *C. caesia* ash. The value of constant C provides the information about the thickness of the boundary layer and the resistance to the external mass transfer.

3.9. Column adsorption study

In the present study, a complicated breakthrough curve was obtained for the adsorption of MG dye. Initially, large amount of surface active sites were available and the dye could be removed completely. Therefore, the values of C_t/C_0 obtained equal to zero during initial 100 min.

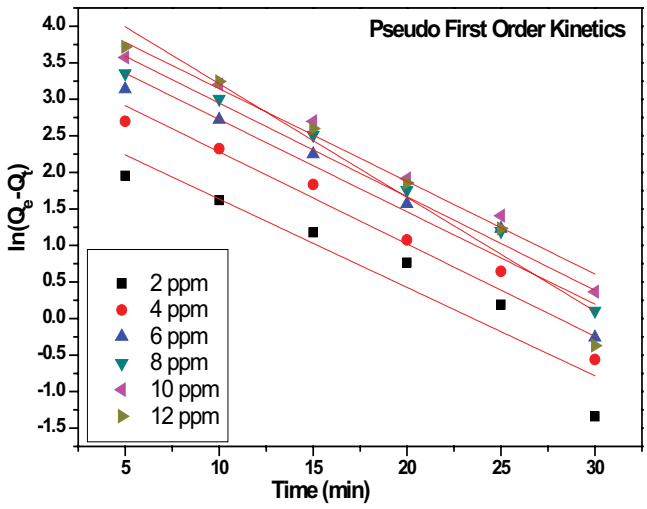

Fig. 11. Linear plot of pseudo-first-order kinetics.

After that different phenomena were occurred. With the occupation of active sites value of C_t/C_0 increased to a maximum of 0.42 at 320 min. Then the values decreased till 630 min and after 630 min a sharp increase was again found upto the value 0.47. Thereafter a decrease in the values was observed. The obtained breakthrough and integrated area are shown in Fig. 14. According to the integral area, the calculated adsorption capacity for present work was found to be 38.16 mg/g (Table 4) which is lower than the batch adsorption capacity.

3.10. Cyclic adsorption desorption study

Regeneration and reuse of an adsorbent is very important for industrial applications. To investigate the recyclable property of *C. caesia* ash 15 mg of the ash was used in the adsorption–desorption recyclability experiment at a constant initial dye concentration of 30 mg/L of MG dye. The exhausted adsorbent was regenerated by simply washing it with distilled water and ethanol followed by

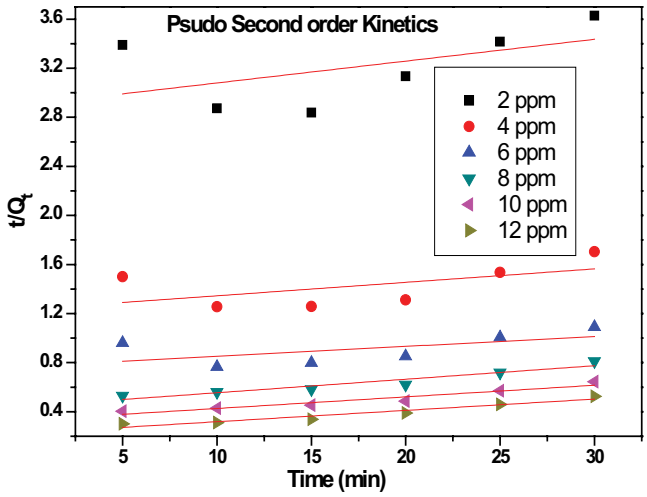

Fig. 12. Linear plot of pseudo-second-order kinetics.

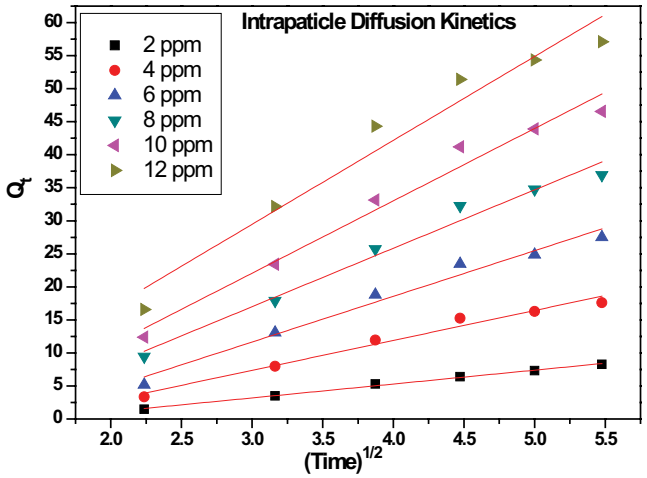

Fig. 13. Linear plot of intraparticle diffusion kinetics.

Table 3
Kinetic parameters for adsorption of malachite green on *Curcuma caesia* ash

Kinetic models	Parameters	Malachite green dye concentration					
		2 ppm	4 ppm	6 ppm	8 ppm	10 ppm	12 ppm
Pseudo-first-order	R^2	0.882	0.956	0.924	0.964	0.971	0.945
	k_1	0.121	0.126	0.126	0.128	0.127	0.156
	Q_e^{cal}	17.188	34.621	54.034	68.708	82.597	117.883
	Q_e^{exp}	8.53	18.18	28.29	38.052	47.995	57.78
Pseudo-second-order	R^2	0.092	0.147	0.19	0.891	0.907	0.919
	k_2	1.09×10^{-4}	9.72×10^{-5}	8.47×10^{-5}	2.73×10^{-4}	2.71×10^{-4}	3.77×10^{-4}
	Q_e^{cal}	56.18	91.24	123.76	90.744	105.485	108.342
	Q_e^{exp}	8.53	18.18	28.29	38.052	47.995	57.78
Intraparticle diffusion	R^2	0.996	0.974	0.974	0.976	0.971	0.948
	k_i	2.1	4.53	6.91	8.84	10.95	12.7
	C	–3.11	–6.235	–9.08	–9.52	–10.78	–8.62

drying in hot air oven at 50°C. The ash of *C. caesia* can be reused up to eight successive cycles without any significant loss in its adsorption efficiency (Fig. 15 and Table 5). With each adsorption–desorption cycle a marginal decrease in percentage removal of the dye was observed and 96% dye removal obtained in first cycle was decreased to 80% till ninth cycle.

Table 4
Parameters of breakthrough curve MG on *Curcuma caesia* ash fixed bed column

Flow rate (mL/min)	1.2
t (min)	865
Peak area (mg/min/L)	7,945.88
q_e (mg/g)	38.16
m_{total} (mg)	10.38
Q_{total} (mg)	9.54
R (%)	91.91

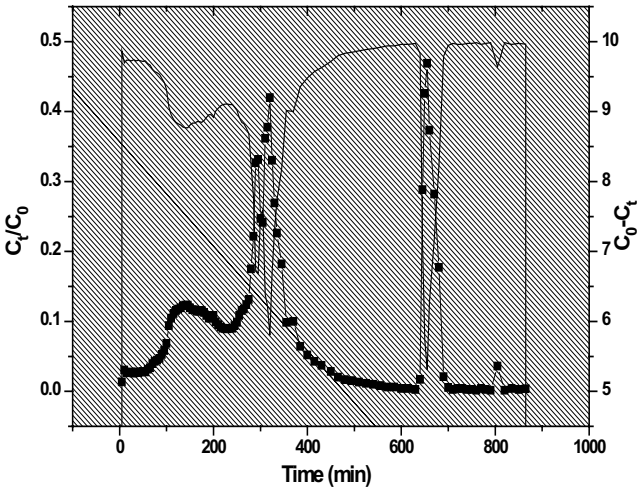

Fig. 14. Breakthrough curve (line, left vertical axis) and integral area (oblique line, right vertical axis) of malachite green on *Curcuma caesia* plant ash fixed bed column.

Table 5
Reusability data of MG removal on to *Curcuma ceasia* ash

S. No.	Number of cycle	Removal efficiency (%)
1	1	96.25
2	2	96.19
3	3	96.11
4	4	95.99
5	5	95.84
6	6	95.65
7	7	95.3
8	8	94.97
9	9	80.53

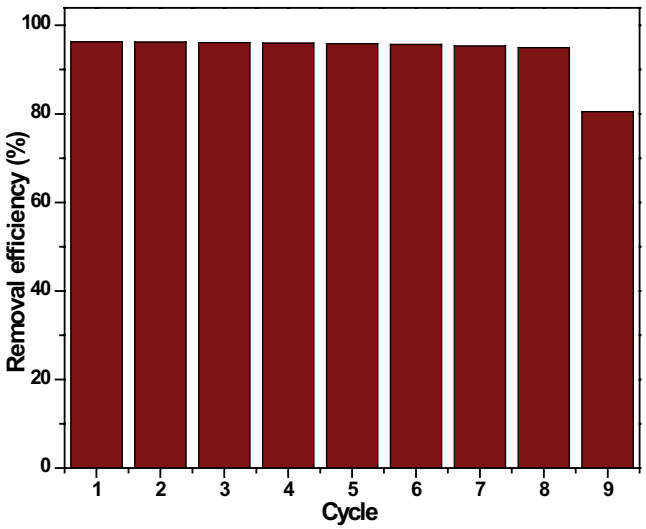

Fig. 15. Adsorption–desorption recyclability of *Curcuma ceasia* ash for MG dye removal.

4. Conclusion

Natural adsorbent *C. caesia* ash was employed for the removal of malachite green dye from aqueous solutions and its adsorption capacity was well-investigated and elucidated. The dye removal was favored in basic medium and at higher temperatures. The MG dye removal process was controlled by physic-sorption mechanism. Intraparticle diffusion model was more suitable for explicating the adsorption data. The adsorption process was spontaneous and endothermic.

References

[1] A. Afkhami, R. Moosavi, Adsorptive removal of Congo red, a carcinogenic textile dye, from aqueous solutions by maghemite nanoparticles, J. Hazard. Mater., 174 (2010) 398–403.
[2] P. Pengthamkeerati, T. Satapanajaru, N. Chatasatapattayakul, P. Chairattanamanokom, N. Sananwai, Alkaline treatment of biomass fly ash for reactive dye removal from aqueous solution, Desalination, 261 (2010) 34–40.
[3] A. Mittal, A. Malviya, D. Kaur, J. Mittal, L. Kurup, Studies on the adsorption kinetics and isotherms for the removal and recovery of methyl orange from wastewaters using waste materials, J. Hazard. Mater., 148 (2007) 229–240.
[4] S. Chen, J. Zhang, C. Zhang, Q. Yue, Y. Li, C. Li, Equilibrium and kinetics studies of methyl orange and methyl violet adsorption on activated carbo derived from *Phragmites australis*, Desalination, 252 (2010) 149–156.
[5] M. Mobarak, E.A. Mohamed, A.Q. Selim, M.F. Eissa, M.K. Seliem, Experimental results and theoretical statistical modelling of malachite green adsorption onto MCM-41 silica/rice husk composite modified by beta radiation, J. Mol. Liq., 273 (2019) 68–82.
[6] V.K. Gupta, R. Jain, A. Mittal, T.A. Saleh. A. Nayak, S. Agarwal, S. Sikarwar, Photo-catalytic degradation of toxic dye amaranth on TiO_2/UV in aqueous suspensions, Mater. Sci. Eng., C, 32 (2012) 12–17.
[7] A. Bhatnagar, M. Sillanpaa, A. Witek-Krowiak, Agricultural waste peels as versatile biomass for water purification – a review, Chem. Eng. J., 270 (2015) 244–271.
[8] Y. Fu, P. Xu, D. Huang, G. Zeng, C. Lai, L. Qin, B. Li, J. He, H. Yi, M. Cheng, C. Zhang, Au nanoparticles decorated on activated

coke via a facile preparation for efficient catalytic reduction of nitrophenols and azo dyes, Appl. Surf. Sci., 473 (2019) 578–588.
[9] L. Qin, D. Huang, P. Xu, G. Zeng, C. Lai, Y. Fu, H. Yi, B. Li, C. Zhang, M. Cheng, C. Zhou, X. Wen, *In-situ* deposition of gold nanoparticles onto polydopamine-decorated g-C_3N_4 for highly efficient reduction of nitroaromatics in environmental water purification, J. Colloid Interface Sci., 534 (2019) 357–369.
[10] C. Arora, S. Soni, S. Sahu, J. Mittal, P. Kumar, P.K. Bajpai, Iron based metal organic framework for efficient removal of methylene blue dye from industrial waste, J. Mol. Liq., 284 (2019) 343–352.
[11] C. Arora, D. Sahu, D. Bharti, V. Tamrakar, S. Soni, S. Sharma, Adsorption of hazardous dye crystal violet from industrial waste using low cost adsorbent *Chenopodium* album, Desal. Water Treat., 167 (2019) 324–332.
[12] X. Yao, Y. Zheng, H. Zhou, K. Xu, Q. Xu, L. Li, Effects of biomass blending, ashing temperature and potassium addition on ash sintering behaviour during co-firing of pine sawdust with a Chinese anthracite, Renewable Energy, 147 (2020) 2309–2320.
[13] X. Yao, H. Zhou, K. Xu, S. Chen, J. Ge, Q. Xu, Systematic study on ash transformation behaviour and thermal kinetic characteristics during co-firing of biomass with high ratios of bituminous coal, Renewable Energy, 147 (2020) 1453–1468.
[14] X. Yao, H. Zhou, K. Xu, Q. Xu, L. Li, Evaluation of the fusion and agglomeration properties of ashes from combustion of biomass, coal and their mixtures and the effects of K_2CO_3 additives, Fuel, 255 (2019) 115829–11840.
[15] I.D. Mall, V.C. Srivastava, N.K. Agarwal, I.M. Mishra, Adsorptive removal of malachite green dye from aqueous solution by bagasse fly ash and activated carbon kinetic study and equilibrium isotherm analyses, Colloids Surf., A, 264 (2005) 17–28.
[16] B.S. Kaith, Sukriti, J. Sharma, T. Kaur, S. Sethi, Uma Shankar, V. Jassali, Microwave assisted green synthesis of hybrid nanocomposite: removal of malachite green from waste water, Iran. Polym. J., 25 (2016) 787–797.
[17] P. Donipati, S.H. Sreeramulu, Preliminary phytochemical screening of *Curcuma caesia*, Int. J. Curr. Microbiol. Appl. Sci., 4 (2015) 30–34.
[18] R. Sahu, J. Saxena, Bioactive compound from Rhizome part of *Curcuma caesia*, Int. J. Pharm. Sci. Rev. Res., 49 (2018) 6–8.
[19] H.P. Devi, P.B. Mazumder, L.P. Devi, Antioxidant and antimutagenic activity of *Curcuma caesia* Roxb. rhizome extracts, Toxicol. Rep., 2 (2015) 423–428.
[20] S. Das, P. Mondal, K. Zaman. *Curcuma caesia* Roxb. and its medicinal uses: a review, Int. J. Pharm. Chem., 3 (2013) 370–375.
[21] A.K. Jain, V.K. Gupta, A. Bhatnagar, Suhas, Utilization of industrial waste products as adsorbents for the removal of dyes, J. Hazard. Mater., 101 (2003) 31–42.
[22] A.K. Jain, V.K. Gupta, A. Bhatnagar, S. Jain, Suhas, A comparative assessment of adsorbents prepared from industrial wastes for the removal of cationic dye, J. Indian Chem. Soc., 80 (2003) 267–270.
[23] J. Song, W. Zou, Y. Bian, F. Su, R. Han, Adsorption characteristics of methylene blue by peanut husk in batch and column modes, Desalination, 265 (2011) 119–125.
[24] V.K. Gupta, Suhas, I. Tyagi, S. Agarwal, R. Singh, M. Chaudhary, A. Harit, S. Kushwaha, Column operation studies for the removal of dyes and phenols using a low cost adsorbent, Global J. Environ. Sci. Manage., 2 (2016) 1–10.
[25] Y. Fu, L. Qin, D. Huang, G. Zeng, C. Lai, B. Li, J. He, H. Yi, M. Zhang, M. Cheng, X. Wen, Chitosan functionalized activated coke for Au nanoparticles anchoring: green synthesis and catalytic activities in hydrogenation of nitrophenols and azo dyes, Appl. Catal., B, 255 (2019) 117740–117746.
[26] L. Qin, Z. Zeng, G. Zeng, C. Lai, A. Duan, R. Xiao, D. Huanga, Y. Fu, H. Yi, B. Li, X. Liu, S. Liu, M. Zhang, D. Jiang, Cooperative catalytic performance of bimetallic Ni-Au nanocatalyst for highly efficient hydrogenation of nitroaromatics and corresponding mechanism insight, Appl. Catal., B, 259 (2019) 118035.
[27] J.X. Yu, J. Zhu, L.Y. Feng, X.L. Cai, Y.F. Zhang, R.A. Chi, Removal of cationic dyes by modified waste biosorbent under continuous model: Competitive adsorption and kinetics, Arabian J. Chem., 12 (2019) 2044–2051.
[28] T.W. Seow, C.K. Lim, Removal of dye by adsorption: a review, Int. J. Appl. Eng. Res., 11 (2016) 2675–2679.
[29] S. Hamidzadeh, M. Torabbeigi, S.J. Shataheri, Removal of crystal violet from water by magnetically modified activated carbon and nanomagnetic iron oxide, J. Environ. Health Sci. Eng., 13 (2015) 8.
[30] P. Qin, Y. Yang, X. Zhang, J. Niu, H. Yang, S. Tian, J. Zhu, M. Lu, Highly efficient, rapid and simultaneous removal of cationic dyes from aqueous solution using monodispersed mesoporous silica nanoparticles as the adsorbent, Nanomaterials, 8 (2018) 1–4, doi: 10.3390/nano801004.
[31] Y. Han, M. Liu, K. Li, Q. Sun, W. Zhang, C. Song, G. Zhang, Z.C. Zhang, X. Guo, *In situ* synthesis of titanium doped hybrid metal-organic framework UiO-66 with enhanced adsorption capacity for organic dyes, Inorg. Chem. Front., 4 (2017) 1870–1880.
[32] J. Fu, Q. Xin, X. Wu, Z. Chen, Y. Yan, S. Liu, M. Wang, Q. Xu, Selective adsorption and separation of organic dyes from aqueous solution on polydopamine microspheres, J. Colloid Interface Sci., 461 (2016) 292–304.
[33] C. Li, X. Wang, D. Meng, L. Zhou, Facile synthesis of low cost magnetic biosorbent from peach gum polysaccharide for selective and efficient removal of cationic dyes, Int. J. Biol. Macromol., 107 (2018) 1871–1878.
[34] X. Zhao, S. Liu, Z. Tang, H. Niu, Y. Cai, W. Meng, F. Wu, J.P. Giesy, Synthesis of magnetic metal organic framework (MOF) for efficient removal of organic dyes from water, Sci. Rep., 5 (2015) 11849.
[35] F. Najafi, O. Moradi, M. Rajabi, M. Asif, I. Tyagi, S. Agarwal, V.K. Gupta, Thermodynamics of the adsorption of nickel ions from aqueous phase using graphene oxide and glycine functionalized graphene oxide, J. Mol. Liq., 208 (2015) 106–113.
[36] X. Ren, D. Shao, S. Yang, J. Hu, G. Sheng, X. Tan, X. Wang, Comparative study of Pb(II) sorption on XC-72 carbon and multi-walled carbon nanotubes from aqueous solutions, Chem. Eng. J., 170 (2011) 170–177.
[37] D. Robati, B. MIrza, M. Rajabi, O. Moradi, I. Tyagi, S. Agarwal, V.K. Gupta, Removal of hazardous dyes-BR 12 and methyl orange using graphene oxide as an adsorbent from aqueous phase, Chem. Eng. J., 284 (2016) 687–697.
[38] H. Li, D.-l. Xiao, H. He, R. Lin, P.-l Zuo, Adsorption behavior and adsorption mechanism of Cu(II) ions on amino-functionalized magnetic nanoparticles, Trans. Nonferrous Met. Soc. China, 23 (2013) 2657−2665.
[39] A. Mittal, J. Mittal, A. Malviya, D. Kaur, V.K. Gupta, Adsorption of hazardous dye crystal violet from wastewater by waste materials, J. Colloid Interface Sci., 343 (2010) 463–473.

Supplementary information

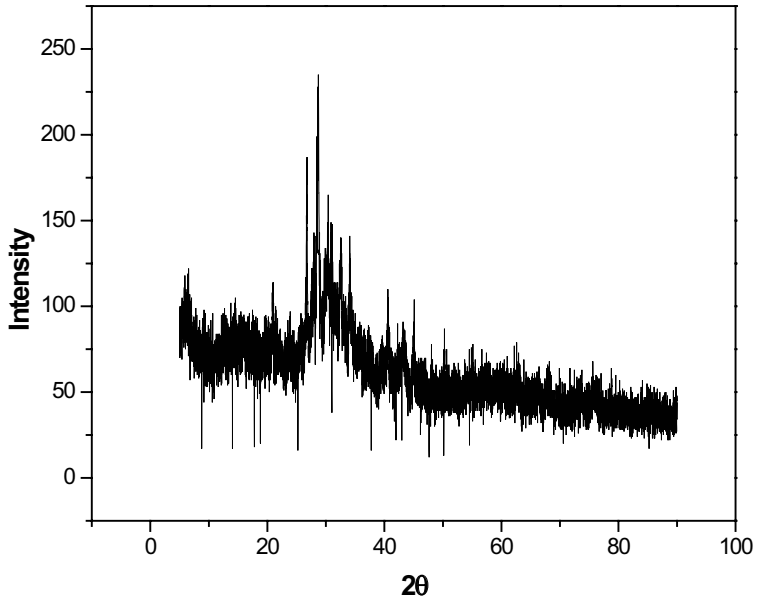

Fig. S1. PXRD pattern of ash of *curcuma caesia*.

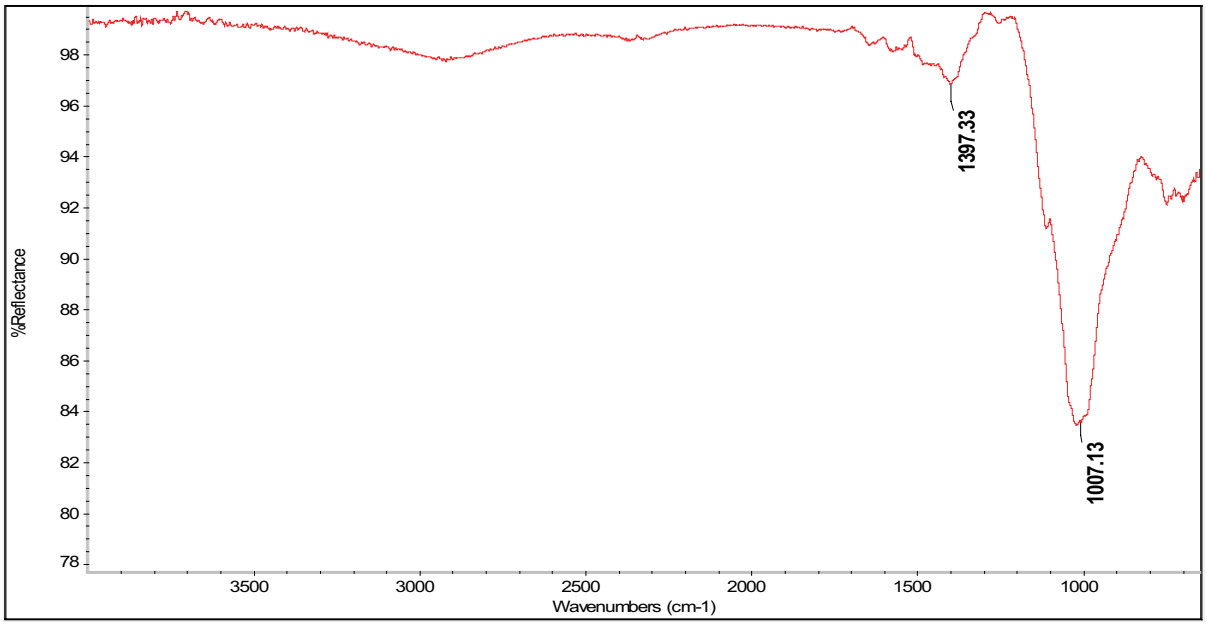

Fig. S2. IR spectra *Curcuma caesia* ash before adsorption.

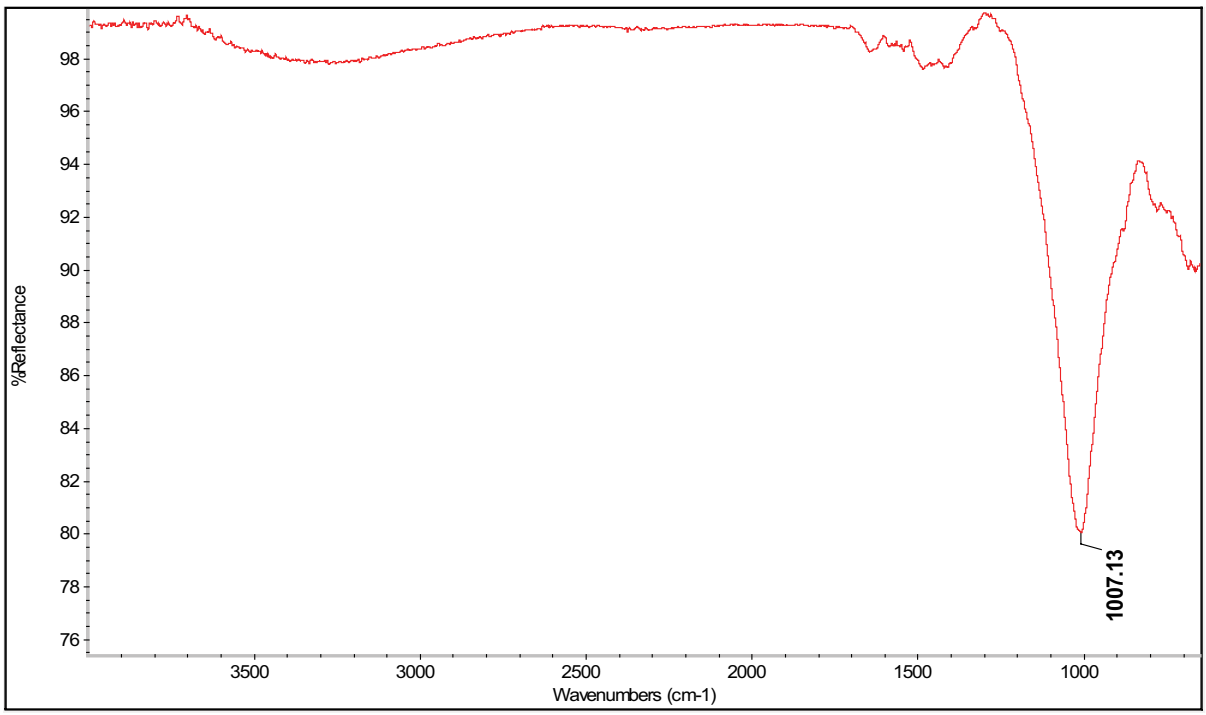

Fig. S3. IR spectra *Curcuma caesia* ash after adsorption.